Identification of a novel interaction between SMC1 DNA damage repair protein and *Escherichia coli* O157: H7 EspF using co-immunoprecipitation combined with mass spectrometry

Muqing Fu
Southern Medical University
Ying Hua
Southern Medical University
Kaina Yan
Southern Medical University
Jia Li
Southern Medical University
Jiali Wu
Southern Medical University
Jinyue Liu
Southern Medical University
Xiaoxia Li
Southern Medical University
Bao Zhang
Southern Medical University
Wei Zhao
Southern Medical University
Qiwei Zhang
Southern Medical University
Chengsong Wan (gzwcs@smu.edu.cn)
Southern Medical University

Research article

Keywords: Enterohemorrhagic Escherichia coli O157: H7, EspF, SMC1, CoIP-MS, protein-protein interactions

Posted Date: August 14th, 2020

DOI: https://doi.org/10.21203/rs.3.rs-19408/v2

Abstract

Background: It is known that the enterohemorrhagic *Escherichia coli* (EHEC) O157: H7 EspF is a multifunctional effector that triggers several damage processes in the host cells. However, in the process of EHEC O157: H7 infection, the interaction between EspF or its N/ C-terminus with host proteins are still unclear.

Results: In this study, we used co-immunoprecipitation combined with mass spectrometry to screen EspF-interacting proteins. A total of 311 host proteins are detected. The N-terminus of EspF is found to interact with 192 proteins, whereas 205 proteins interact with the C-terminus of EspF. These proteins are mainly involved in RNA splicing, endoplasmic reticulum stress, and a variety of metabolic signaling pathways. We verify for the first time that SMC1 interacts with EspF and more likeliy by its C-terminus, and provide evidence that EspF increases p-SMC1 levels. p-SMC1, known to reduce the S-phase cell cycle arrest and DNA damage repair. Surprisingly, we screen that EspF can also phosphorylate H2AX, suggesting that EspF may directly mediate DNA damage through SMC1 phosphorylation.

Conclusion: Taken together, this is the first study describing the interaction between EspF and SMC1. Our work lays a foundation for further research on directly EspF-mediated host cells' DNA damage, apoptosis, and even colorectal carcinogenesis.

Background

Enterohemorrhagic *E. coli* O157: H7 is an important foodborne pathogen that causes human diarrhea, hemorrhagic colitis, hemolytic uremic syndrome, and thrombotic thrombocytopenic purpura. Severe cases may be life-threatening. EHEC O157: H7 uses the T3SS type III secretion system to adhere to the brush border of epithelial cells, and then injects effector proteins into host cells. EspF is one of the most important virulence factors of A / E pathogens (M & P, 2014). EspF exists in EHEC, enteropathogenic *Escherichia coli* (EPEC), and *Citrobacter rodentium*, which are potentially harmful to human. It targets the mitochondria and nucleoli(Nougayrède & Donnenberg, 2004, Dean et al., 2010), destroys the tight junctions of intestinal epithelial cells (Weflen et al., 2010), leading to the cytoskeletal rearrangement and disappearance of intestinal epithelial microvilli, and induces host cell apoptosis (Zhao, 2010). Due to its biological effects, it is known as the "Swiss Army Knife" of bacterial pathogens (Holmes et al., 2010).

The N-terminus of EHEC O157: H7 EspF (1-73 aa) contains a secretion signal (1-20 aa), a host cell mitochondrial targeting signal (mitochondrial targeting signal, MTS, 1-24 aa) (Charpentier & Oswald, 2004), and a nucleus-binding domain (Nucleolar targeting domain, NTD, 21-74aa)(Dean *et al.*, 2010). Roxas found that EspF localizes to mitochondria, destroys mitochondrial membrane potential, and activates the apoptotic proteases 3 and 9. The apoptotic proteases can cleave the epidermal growth factor receptor (EGFR) of host cells, leading to the degradation of EGFR and a dramatic increase in host cell death in the late stages of infection (Roxas et al., 2007). The C-terminus (73-248 aa) is composed of four highly homologous proline-rich sequences(PRRs), each containing a eukaryotic cell SNX9 (Sorting nexin 9), protein binding site SH3 (Src homology 3) motif, and an N-WASP (Neuronal Wiskott-Aldrich syndrome protein) binding domain, a possible actin-binding motif (Holmes *et al.*, 2010, Mcnamara & Donnenberg, 2006). In addition, the results of Amin shows that EspF has a particular anti-phagocytosis effect. The EspF of EHEC O26: H11 and EPEC O127: H6 can prevent bacteria from being engulfed by macrophages by the PI3K pathway, while the ability of EspF in O157: H7 is significantly reduced (Tahoun, 2011).

Although there has been some research on the interaction between EspF and host proteins, the molecular mechanisms of EspF interaction with host proteins and the impact of these interactions on cell damage and apoptosis are still unclear. The identification of the interaction between EspF and the host is important to elucidate the pathogenic mechanism.

CoIP-MS is one of the most widely used high-throughput techniques for discovering protein-protein interactions. In our research, we analyzed the molecular function (MF), biological processes (BP) and cellular components (CC) of the related proteins by Gene Ontology (GO), Kyoto Encyclopedia of Genes and Genomes (KEGG), and Clusters of Orthologous Groups (COG) functional annotations. The STRING online tool was used to analyze interactions between target proteins, and Cytoscape software was used to draw the protein interaction network (PPI). The interactions were validated by immunoprecipitation, and co-localization of EspF and the target proteins was performed by confocal microscopy. The protein expression were identified. Our research provided a protein network map between EspF and the host proteins, laying a foundation for further research on how EspF directly mediates DNA damage in the host cells, even causes colorectal carcinogenesis.

Results

Isolation of differential bands in EspF / EspF-N / EspF-C groups from cell lysates

After transfecting pEGFP-EspF, pEGFP-EspF / N, and pEGFP-EspF / C-terminus encoding plasmids into 293T cells for 48 hours, the lysis proteins were added to Flag columns and IgG columns for co-immunoprecipitation (Figure 1). pEGFP-EspF was about 58 kDa, pEGFP-EspF / N was 33 kDa, and pEGFP-EspF / C was 55 kDa. Compared with the IgG group, between 35-40 kDa, there were two differentially expressed bands in the pEGFP-EspF group. at 40 kDa, there was a differential band in the pEGFP-EspF / N group. At 120 kDa, there was a differential band in the pEGFP-EspF / C group. Besides these bands, the bands at the same position in the lanes of the respective IgG groups were also cut out. The bands were digested by mass spectrometry to detect the interacting proteins, and the Flag group-specific proteins (minus the IgG group proteins) were considered as the putative interacting proteins.

Prediction and analysis of interacting protein with EspF

A total of 708 proteins were identified in this work, 311, 192, and 205 proteins were detected in the pEGFP-EspF group, pEGFP-EspF / N group, and pEGFP-EspF / C group, respectively. We also performed functional annotation (including GO, Pathway, STRING analysis) to identify proteins. Through these analyses, we attempted to discover essential proteins.

All possible target proteins that interacted with EspF were loaded into the DAVID database for KEGG pathway annotation and GO enrichment. The threshold was set to ps0.05, and pathways or gene functions with higher counts were analyzed. The top 20 pathways were plotted with Graphpad Prism 6 (Table 1). Analysis of the differential bands at about 38 kDa in the pEGFP-EspF group by GO annotation analysis revealed that the interacting proteins were involved in 25 biological processes (BPs). Of these, the primary were intracellular processes (12.3%), metabolic processes (10.9%), biological regulation (8.8%), and immune stimulation (6.6%). Cell Components (CCs) enrichment mainly involved cellular anatomical entities (37.7%), intracellular (36.6%), and protein-containing complex (20.9%). Molecular Functions (MFs) mostly involved binding (53.6%) and catalytic activity (22.3%) (Figure 2A). Pathway analysis showed that the interacting proteins involved 183 pathways, notably metabolic pathways (32.6%), carbon metabolism (19.6%), and biosynthesis of amino acids (13.0%). (Figure 2B).

We used STRING to analyze the target proteins with which EspF interacted, and found that RPS6, RPL14, and EIF2S1 had the highest connectivity (Figure 2C). RPS6 plays an essential role in controlling cell growth and proliferation by selectively translating specific kinds of mRNAs (Meyuhas, 2015). RPL14 is a large ribosomal subunit component that plays a role in mRNA catabolism and translation (Enerly et al., 2003). EIF2S1 works in the early stages of protein synthesis by forming a ternary complex with GTP and initiator tRNA (Boye & Grallert, 2019). This analysis showed that in addition to gene transcription regulation and protein synthesis, EspF also plays a crucial role in cell proliferation, and catabolism.

The GO annotation analysis of the 36 kDa differential band showed that the interacting proteins were involved in 26 BPs, such as intracellular processes (12.5%), metabolic processes (10.2%), and biological regulation (9.0%). CCs and MFs results were consistent with the 38 kDa differential band results (Figure 3A). Pathway analysis showed that the interacting proteins involved 150 pathways, including metabolic pathways (23.0%), protein processing in the endoplasmic reticulum (13.1%) (Figure 3B). STRING analysis showed that RPL7A, RPS20, and EIF2S1 had a high degree of connectivity, and we found that there was also a high degree of connectivity between the MDH2 and GOT2 (Figure 3C). Among them, MDH2 plays a role in cell metabolism and amino acid acetylation (Gabay-Maskit et al., 2018). GOT2 is necessary for metabolite exchange between mitochondria and cytoplasm and plays a crucial role in amino acid metabolism (Yang et al., 2018).

Rank	Protein symbol	Protein annotation
1	NP_312577.1	T3SS secreted effector EspF [*Escherichia coli* O157:H7 str. Sakai]
2	sp|P21796|VDAC1_HUMAN	Voltage-dependent anion-selective channel protein 1 OS = Homo sapiens OX 9606 GN=VDAC1 PE=1 SV=2
3	sp|O00165|HAX1_HUMAN	HCLS1-associated protein X-1 OS=Homo sapiens OX=9606 GN=HAX1 PE=1 SV=2
4	sp|P36542|ATPG_HUMAN	ATP synthase subunit gamma, mitochondrial OS=Homo sapiens OX=9606 GN=ATP5F1C PE=1 SV=1
5	sp|Q9Y623|MYH4_HUMAN	Myosin-4 OS=Homo sapiens OX=9606 GN=MYH4 PE=2 SV=2
6	sp|Q13347|EIF3I_HUMAN	Eukaryotic translation initiation factor 3 subunit I OS=Homo sapiens OX=9606 GN=EIF3I PE=1 SV=1
7	sp|Q15006|EMC2_HUMAN	ER membrane protein complex subunit 2 OS=Homo sapiens OX=9606 GN=EMC2 PE=1 SV=1
8	sp|Q01449|MLRA_HUMAN	Myosin regulatory light chain 2, atrial isoform OS=Homo sapiens OX=9606 GN=MYL7 PE=1 SV=1
9	sp|P17661|DESM_HUMAN	Desmin OS=Homo sapiens OX=9606 GN=DES PE=1 SV=3
10	sp|Q9P035|HACD3_HUMAN	Very-long-chain (3R)-3-hydroxyacyl-CoA dehydratase 3 OS=Homo sapiens OX=9606 GN=HACD3 PE=1 SV=2
11	sp|P60709|ACTB_HUMAN	Actin, cytoplasmic 1 OS=Homo sapiens OX=9606 GN=ACTB PE=1 SV=1
12	sp|P35613|BASI_HUMAN	Basigin OS=Homo sapiens OX=9606 GN=BSG PE=1 SV=2
13	sp|P60891|PRPS1_HUMAN	Ribose-phosphate pyrophosphokinase 1 OS=Homo sapiens OX=9606 GN=PRPS1 PE=1 SV=2
14	sp|Q07955|SRSF1_HUMAN	Serine/arginine-rich splicing factor 1 OS=Homo sapiens OX=9606 GN=SRSF1 PE=1 SV=2
15	sp|Q13505|MTX1_HUMAN	Metaxin-1 OS=Homo sapiens OX=9606 GN=MTX1 PE=1 SV=3
16	sp|P05976|MYL1_HUMAN	Myosin light chain 1/3, skeletal muscle isoform OS=Homo sapiens OX=9606 GN=MYL1 PE=2 SV=3
17	sp|Q96FZ7|CHMP6_HUMAN	Charged multivesicular body protein 6 OS=Homo sapiens OX=9606 GN=CHMP6 PE=1 SV=3
18	sp|P62424|RL7A_HUMAN	60S ribosomal protein L7a OS=Homo sapiens OX=9606 GN=RPL7A PE=1 SV=2
19	sp|P35232|PHB_HUMAN	Prohibitin OS=Homo sapiens OX=9606 GN=PHB PE=1 SV=1
20	sp|P10599|THIO_HUMAN	Thioredoxin OS=Homo sapiens OX=9606 GN=TXN PE=1 SV=3

Table 1 The top 20 proteins of the 38 kDa differential band between the EspF group and IgG group.

Prediction and analysis of interacting proteins with EspF-N or C-terminus

The GO annotation analysis of the differential bands at about 40 kDa in the pEGFP-EspF / N group showed that 228 interacted proteins involved 25 BPs, such as intracellular processes (12.3%), metabolic processes (10.8%), and biological regulation (9.2%). The CCs and MFs analyses were similar to EspF-interacted proteins. Pathway analysis revealed interacted proteins were mainly involved in metabolic pathways (27.1%), protein processing in the endoplasmic reticulum

(9.41%), and pathways in cancer (8.2%). (Figure 4A and B). STRING analysis of target proteins interacting with EspF-N terminus also found that RPL8, RPS9, and EIF3I proteins had the highest degree of connectivity, indicating that EspF may use its N-terminus for ribosomes recognize binding sites (Figure 4C).

GO annotation analysis of the pEGFP-EspF / C group in the 120 kDa differential band showed that BPs enrichment mostly involved translation (23.1%), oxidation-reduction process (15.4%), and intracellular protein transport (13.5%). CCs enrichment mainly involved intermediate filament (21.3%), ribosome (13.5%). MFs mostly involved protein binding (22.4%), and ATP binding (18.6%) (Figure 5A). Of the interacted proteins, 30.3% were localized in the cytoplasm, and 27.27% were localized in the nucleus (Figure 5B). COG analysis showed that interacted proteins mostly involved translation, ribosomal structure, biogenesis, posttranslational modification (Figure 5C). KEGG showed that most of the cellular processes involved protein transport, and the signal generation that affected cell growth and apoptosis (Figure 5D). Among these proteins, TUBB, and ANXA2 showed strong interaction with EspF-C. TUBB, a main component of tubulin, has GTPase activity, and plays a key role in the microtubule cytoskeleton organization (Ti et al., 2018). Studies have shown that EspF interacts with SNX9 to induce the formation of membrane tubules and the host cell membrane change (Marches et al., 2006). In addition to the SNX9 binding site, EspF can also activate N-WASP to induce actin polymerization, and TJ disruption (Garber et al., 2018). Moreover, EspF also directly binds to cytokeratin 18, which contributes to the collapse of the cytoskeleton(Viswanathan et al., 2004). Microfilaments, microtubules, and intermediate fibers together make up the cytoskeletal system. Therefore, we speculated that EspF might also cause cytoskeleton rearrangement by binding TUBB .

In our previous research, ANXA6 and EspF were confirmed to interact(Hua et al., 2018). This time we found ANXA2, a member of the ANXA protein family, which is a calcium-regulated membrane-bound protein. ANXA2 participates in the heat stress response by interacting with Hsp90 (Díaz-Díaz et al., 2020). Meanwhile, EspF may regulate calcium ion accumulation and calcium channel protein activity by interacting with ANXA2.

In addition, we also found the SMC family proteins. The interaction between EspF and SMC1 is also found in our previous research and involves multiple signaling pathways (Hua *et al.*, 2018). It is understood that SMC1 is a chromosomal structural protein that plays a role in DNA replication and cohesion of sister chromatids. It involves in chromosome dynamics, cell cycle regulation, cell proliferation, and genome stability (Li et al., 2019). Furthermore, when cells were stimulated by DNA damage, SMC1 can be phosphorylated by ATM or ATR to participate in DNA repair and acted as a downstream effector in the ATM / NBS1 and the ATR / MSH2 branch to active S-phase checkpoint (Lidza et al., 2014). Hence, we hypothesized EspF could mediate cellular DNA damage repair by phosphorylating SMC1.

SMC1 was identified as a novel EspF-interacting protein, and its interaction was by EspF-C terminus

We are the first to study the mechanism of interaction between EspF and DNA damage repair proteins. Western blotting and confocal analysis further confirmed the interaction between EspF and SMC1. Co-immunoprecipitation results confirmed that EspF interacted with SMC1, and the interaction was more stronger with EspF-C terminus (Figure 6A). Immunofluorescence analysis also showed that EspF and SMC1 were co-localized in the cytoplasm (Figure 6B), and EspF relocated SMC1 more from the nucleolus into the cytoplasm, suggesting that SMC1 may not play its usual role in the nucleolus.

To investigate the interation of EspF and SMC1, we measured SMC1 and its phosphorylation levels after transfected EspF into Caco2 cells. Immunofluorescence showed that compared with the control, the level of SMC1 remained unchanged after transfection with EspF, but p-SMC1 significantly increased (Figure 6C), and p-SMC1 was distinctly localized in the cytoplasm and co-localized with EspF (Supplementary material). We then verified the results by infecting HT-29 cells with the strain. The expression of p-SMC1 in cells transfected with the EDL 933 was higher than infected *ΔespF* strain, and infecting the complement *ΔespF / pespF* restored p-SMC1 expression. The above results verified that EspF could increase the expression level of p-SMC1.

In general, when the host DNA is damaged, cyclin-mediated cell cycle arrest will occur. During this period, DNA damage repair proteins are recruited to double side-band break (DSB) (Jackson & Bartek, 2009). Therefore, we speculated that EspF might lead to DNA damage, which stimulates the S-phase detection point by increases p-SMC1 expression, thus mediating damage repair.

EspF may mediate DNA damage by modifying the histones

Mass spectrum results showed that EspF could modify multiple sites of various proteins (Table 2). Among the modification results, SFXN1, HAX1, EIF3I, ATG16L1, and DNA damage binding proteins had high scores. SFXN1 is a mitochondrial serine transporter that mediates serine into mitochondria and plays an essential role in the single-carbon metabolic pathway(Kory et al., 2018). EspF can cause oxidative phosphorylation and methylation of SFXN1, which may mediate the metabolism required component for transport in and out of the mitochondria. HAX1 recruits the Arp2 / 3 complex to the cell cortex, and through its interaction with KCNC3, it reconstitutes the cortical actin cytoskeleton(Zhang et al., 2016). EspF may rearrange the cytoskeleton and modulate cell survival through phosphorylation and acetylation of the HAX1. EIF3I is a part of the EIF-3 complex and uses different RNA stem-loop binding modes to increase ERK translation(Zhang et al., 2017). EspF may act on the translation of mRNA involved in cell proliferation (including cell cycle, differentiation, and apoptosis) through phosphorylation and acetylation of EIF3I. EspF may also phosphorylate some autophagy-related proteins, including ATG16L1 and PHB, that mediate BPs such as cell autophagy and protein transport(Jefferson et al., 2020).

We also discovered that EspF could modify a series of histones, such as Histone H1.3, Histone H2A type 1, and Histone H1x, which are the core components of nucleosomes. Nucleosomes encapsulate DNA into chromatin, limiting DNA's entry into cellular mechanisms(Pardal et al., 2019). Therefore, histone modifications play a central role in transcription regulation, DNA damage repair, DNA replication, and chromosomal stability. DNA accessibility is also regulated by a complex set of posttranslational modifications of histones and nucleosome remodeling(Sawan & Herceg, 2010). EspF may affect epigenetic changes in host cells. Importantly, we found that EspF could phosphorylate histone H2AX, a known marker of DNA damage(Nagelkerke & Span, 2016), suggesting that EspF can directly cause DNA damage.

Next, we discovered that EspF also modified the damage-specific DNA-binding protein 2 (DDB2), a kind of DNA repair protein. DDB2 is originally identified as a DNA damage recognition factor that promotes genomic nucleotide excision repair (GG-NER) in human cells. DDB2 is also involved in chromatin remodeling,

gene transcription, cell cycle regulation. Recently, the potential of DDB2 in the development and progression of various cancers has been described. DDB2 activity occurs in several stages of canceration, including cancer cell proliferation, survival, invasion, and cancer stem cell formation(Gilson et al., 2019). Previous research showed that EspF could cause cell apoptosis by targeting mitochondria and releasing cytochrome c(Nougayrède & Donnenberg, 2004), but it is still unclear whether EspF can mediate DNA damage through nuclear modification of histones in the early period, which lays the foundation for our future research.

Table 2 EspF-mediated phosphorylation, acetylation, and methylation of the host proteins.

	Protein symbol	Score	Pep before	Pep_seq	Pep after	Pep mod
1	sp|Q9H9B4|SFXN1_HUMAN	270	R	ILMAAPGMAIPPFIMNTLEK	K	2 Oxidation (M); Phospho (ST); Methyl (K)
2	sp|P09651|ROA1_HUMAN	267	K	SESPKEPEQLR	K	Phospho (ST)
3	sp|P05388|RLA0_HUMAN	187	K	EDLTEIR	D	Phospho (ST)
4	sp|P05388|RLA0_HUMAN	187	R	GNVGFVFTK	E	Phospho (ST); Acetyl (K)
5	sp|P05388|RLA0_HUMAN	187	K	CFIVGADNVGSK	Q	Phospho (ST)
6	sp|A0A075B6P5|KV228_HUMAN	172	R	FSGSGSGTDFTLK	I	Phospho (ST)
7	sp|O00165|HAX1_HUMAN	145	K	ITKPDGIVEERR	T	Phospho (ST); Acetyl (K)
8	sp|Q13347|EIF3I_HUMAN	115	K	QLALLKTNSAVR	T	Phospho (ST); Acetyl (K)
9	sp|Q01449|MLRA_HUMAN	112	K	VSVPEEELDAMLQEGK	G	Phospho (ST); Methyl (K)
10	sp|P35613|BASI_HUMAN	89	K	GSDQAIITLRVR	S	2 Phospho (ST); Methyl (R)
11	sp|P11908|PRPS2_HUMAN	89	K	IASSSRVTAVIPCFPYAR	Q	3 Phospho (ST); Phospho (Y); 2 Methyl (R)
12	sp|P60891|PRPS1_HUMAN	78	K	IASASRVTAVIPCFPYAR	Q	Phospho (ST); Phospho (Y); Methyl (R)
13	sp|Q13505|MTX1_HUMAN	72	K	YNADYDLSAR	Q	Phospho (Y)
14	sp|P35232|PHB_HUMAN	70	R	SRPRNVPVITGSK	D	Phospho (ST); Methyl (R); Acetyl (K)
15	sp|Q99880|H2B1L_HUMAN	65	K	AVTKYTSSK	-	Phospho (ST); Phospho (Y); 2 Methyl (K)
16	sp|Q92522|H1X_HUMAN	64	K	AAKPSVPK	V	Phospho (ST); Methyl (K); Acetyl (K)
17	sp|Q86V81|THOC4_HUMAN	58	-	MADKMDMSLDDIIK	L	2 Oxidation (M); Phospho (ST); Methyl (K)
18	sp|P0C0S8|H2A1_HUMAN	48	K	KTESHHK	A	Phospho (ST); Acetyl (K)
19	sp|P16104|H2AX_HUMAN	48	K	TSATVGPKAPSGGK	K	2 Phospho (ST); Methyl (K)
20	sp|Q8IUE6|H2A2B_HUMAN	48	K	KTESHKPGK	N	Phospho (ST); Methyl (K); 2 Acetyl (K)
21	sp|Q9Y375|CIA30_HUMAN	48	R	KFSKPTSALYPFLGIR	F	Phospho (ST); Acetyl (K)
22	sp|O14983|AT2A1_HUMAN	46	K	EYEPEMGKVYR	A	Oxidation (M); Phospho (Y)
23	sp|Q9Y394|DHRS7_HUMAN	46	K	LGVSLVLSAR	R	Phospho (ST); Methyl (R)
24	sp|P08758|ANXA5_HUMAN	45	R	VMVSRSEIDLFNIR	K	Oxidation (M); Phospho (ST)
25	sp|Q5JTV8|TOIP1_HUMAN	41	K	TPQEWAPQTAR	I	2 Phospho (ST)
26	sp|P10412|H14_HUMAN	40	K	ATGAATPK	K	Phospho (ST)
27	sp|P16402|H13_HUMAN	40	K	KAASGEGKPK	A	Phospho (ST)
28	sp|P22492|H1T_HUMAN	40	K	KPRATTPK	T	Phospho (ST); Acetyl (K)
29	sp|Q02539|H11_HUMAN	40	K	KPKTVKPK	K	Phospho (ST)
30	sp|P16403|H12_HUMAN	40	K	AGGTKPK	K	Phospho (ST); Methyl (K)
31	sp|Q9UFE4|CCD39_HUMAN	37	R	SPSHTSLSAR	S	Phospho (ST)
32	sp|Q9Y4L1|HYOU1_HUMAN	37	K	FTKPRPRPK	D	Phospho (ST); Methyl (K)
33	sp|P31944|CASPE_HUMAN	36	R	LALILCVTK	A	Phospho (ST); Acetyl (K)
34	sp|P07355|ANXA2_HUMAN	36	R	KGTDVPK	W	Phospho (ST); Acetyl (K)
35	sp|P07355|ANXA2_HUMAN	36	K	GTDVPKWISIMTER	S	Oxidation (M); Phospho (ST); Methyl (R); Acetyl (K)
36	sp|P07355|ANXA2_HUMAN	36	K	GTDVPKWISIMTER	S	Oxidation (M); 2 Phospho (ST); Methyl (R)
37	sp|P07355|ANXA2_HUMAN	36	K	LSLEGDHSTPPSAYGSVK	A	Phospho (ST); Methyl (K)
38	sp|Q92466|DDB2_HUMAN	34	K	VTHVALNPCCDWFLATASVDQTVK	I	3 Phospho (ST)
39	sp|Q8WV16|DCAF4_HUMAN	34	R	MGFNASSMLRK	S	Phospho (ST); Methyl (K)
40	sp|Q676U5|A16L1_HUMAN	34	K	CGSDWTR	V	Phospho (ST)

Discussion

Previous studies screened host proteins with EspF interactions mainly through yeast two-hybrid and BiFC fluorescence methods(Hua *et al.*, 2018; Nougayrède et al., 2007). The former cannot determine whether the interactions exist in mammalian cells, while the latter use tags that may affect the conformation or activity of the mark protein, leading to false-negative results. Therefore, we opted for a classic CoIP-MS assay to screen host proteins that interact with EspF in 293T cells. MS results identified 311 proteins. We then analyze the BPs, MFs, and CCs of the interacting proteins by GO enrichment, KEGG pathway, and STRING analyses.

Previous studies have shown that EspF can interact with some proteins. Oliver Marche's identified that SNX9 can bind EPEC EspF via its amino-terminal SH3 region(Oliver et al., 2006), and VK Viswanathan have shown that EspF can interact with the host intermediate filament protein cytokeratin 18 (CK18) in a complex with adaptor protein 14-3-3 epsilon, which can alter the architecture of the intermediate filament network(Viswanathan et al., 2010). Moreover, Hua Ying have found that EspF has the ability to interact with featured ribosomal proteins and to modulate the antiphagocytosis process by bonding with ANXA6(Hua et al., 2018b). In our study, we found that SNX9, SNX18, 14-3-3 epsilon, ANXA6, ANXA2 and EHEC O157:H7 EspF proteins also interact.

MS results showed that host proteins interacting with EspF were mostly involved in metabolic pathways and localized in the cytoplasm and nucleolus. We found that EspF interacted strongly with ribosomal RPL, RPS, and EIF family proteins, and EspF can phosphorylate them. Previous proteomics studies have shown that many ribosomal protein levels in intestinal cells decrease after EPEC infection(Hardwidge et al., 2004). In cells expressing EspF, pre-rRNA synthesis is blocked. At the same time, EspF-dependent EPEC infection reduces the expression level of ribosomal protein RPL9, and changes the relocation of RPS5 and U8 small nucleolar RNA (snoRNA)(Dean et al., 2010). Our results provided further support to the hypothesis that EspF may exercise its biological function by regulating ribosomal protein synthesis and relocation. Future research will attempt to decipher the mechanism by which EspF leads to the inhibition of ribosome synthesis.

EspF targets mitochondria and regulates the expression of DNA mismatch repair proteins in host cells through post-transcriptional manipulation, leading to depletion of Apc and MMR proteins in host cells(Maddocks et al., 2009), and increases the instability of microsatellite DNA sites, which is a precursor to DNA damage and can even lead to colon cancer(Maddocks et al., 2013). In this work, we also found that EspF can lead to H2AX phosphorylation and modify DDB2. Phosphorylated H2AX is an indicator of DNA damage. This series of evidence suggests that when EspF enters the host cell, it may cause DNA damage in the early stage by regulating the expression of damage repair proteins. SMC1 is a chromosomal structural protein. When DNA is damaged, the upstream ATM will phosphorylate SMC1 in DSB to form the BRCA1-NBS1-MRE11 complex, and p-SMC1 activates the S-phase checkpoint in DNA damage repair(Luo et al., 2013). Abnormal SMC1 expression or mutation can lead to a deficient DNA damage repair pathway, which are closely related to tumorigenesis(Ying et al., 2018). Thus, we focused on the interaction between EspF and SMC1. Immunofluorescence and co-immunoprecipitation results confirmed the interaction, and more likely by EspF-C terminus.

Furthermore, EspF can increase the expression of p-SMC1 in $Caco_2$ and HT-29 cells, we hypothesised EspF may lead SMC1 in the nucleus more localized in the cytoplasm and phosphorylate it, resulting in a decrease in chromosomal structural proteins in the nucleus, which decreases the ability of DNA damage repair, and further mediating DNA damage. Thus, EspF may mediate DNA damage repair, cell proliferation, and even canceration by phosphorylating SMC1 (Figure 7). There is already the evidence that *E. coli* infects intestinal epithelial cells, causing DNA damage in host cells, and accelerates NF-κB pathway, and other cellular inflammation pathways(Kipanyula et al., 2013). However, there is no research on whether EspF can directly cause DNA damage, which is worthy of further study.

Meanwhile, we separately studied the interacted proteins and pathogenic mechanisms of EspF-N/C terminus. We found that the proteins interacting with the N-terminus are mostly involved in metabolic pathways and protein processing in the endoplasmic reticulum. Our previous research proved that the N-terminus is essential for cell apoptosis, inflammatory response, and animal toxicity(Wang et al., 2017). Thus, we speculate that EspF-N may also mediate apoptosis through endoplasmic reticulum stress. Previous studies have shown that the EspF-C terminus can bind to various host protein motifs. We were the first to find that the EspF-C terminus can interact with the SMC1, a DNA damage repair protein, which provides a new basis for future studies on DNA damage, microsatellite instability, and even colon cancer caused by EspF.

It is undeniable that CoIP-MS has certain limitations in the screening process. First, the bands for mass spectrometry should be distinct, and some weak interactions may not be detected. Second, different levels of protein expression between different cells may affect the binding efficiency of co-immunoprecipitation. Third, CoIP-MS detects transient effects, so it is not possible to screen all host proteins that interact with EspF. We need further experiments to verify the real interactions.

The host proteins interacted with EspF screened by our research may directly interact with EspF or form multiple subcomplexes with EspF. Furthermore, we confirmed that EspF interacted with SMC1, most likely through its C terminus. At the same time, EspF can increase the p-SMC1 expression level and relocate SMC1 into the cytoplasm. This provides us with new insights into the role of EspF in mediating DNA damage repair. Further research is needed on what processes EspF is involved in and how these effects mediate the bacterial-host pathogenesis. Our screening provides directions for future analysis of the potential biological role of EspF and its N and C terminus.

Conclusion

In this study, we focused on 311 host proteins that interact with the EHEC O157: H7 EspF and used bioinformatics enrichment to analyze their molecular functions, BPs, and cellular pathways. These findings provide new candidates for EspF interactions, suggesting that EspF can phosphorylate H2AX and regulate the DNA damage repair process by interacting with SMC1. These results are very encouraging, and we provided a PPI network of interactions of EspF with the host, which brings great hope for the field of protein interactions mediating the pathogen EHEC O157: H7 and host cell interplay.

Methods

Cell lines and strains

293T, $Caco_2$, and Vero cells were cultured overnight in DMEM (Gibco) containing 10% fetal bovine serum (FBS), 1% penicillin and streptomycin at 5% CO_2 and 37°C. HT-29 cells were cultured overnight in RPMI-1640 (Gibco) medium containing 10% FBS and 1% penicillin and streptomycin at 5% CO_2 and 37°C. The pEGFP-N1 plasmid, strain EHEC O157: H7 EDL 933, *ΔespF,* and *ΔespF / pespF* were stored in our laboratory(Wang *et al.*, 2017). DH5α competent cells and LA

high-fidelity enzyme were purchased from TaKaRa. Restriction enzymes EcoR I and BamH I were purchased from Thermo Fisher Scientific. The primers used in this study were synthesized by Sangon Biotech (Shanghai, China). Gene sequencing was performed by Guangzhou IGE Biotechnology.

Construction of pEGFP-EspF, pEGFP-EspF / N, and pEGFP-EspF / C-terminus encoding plasmids

We amplified the *espF* gene and its N-terminus (1-219 bp) and C-terminus (220-747 bp) with LA high-fidelity enzyme on the genome of EDL 933. Each constructed plasmid was labeled with 3xFlag. Primer *espF-F*: CCGGAATTCGCCACCATGCTTAATGGAATTAGTAACGCTG

and *espF-R*:

CGCGGATCCCCGCTACCGCCGCTTCCCTTGTCCTTATCGTCGTCATCCTTGTAATCCTTATCGTCGTCATCCTTGTAATCCTTATCGTCGTCATCCTTGTAATCCCCTTTCT amplified the *espF* gene; primer *espF / N-F*: CCGGAATTCGCCACCATGCTTAATGGAATTAGACAC

and *espF / N-R*: CGCGGATCCCCACCAGAGCCACCCTTATCGTCGTCATCCTTGTAATCGGGAGTAAATGAAGTCACCTG amplified the *espF / N*; primer *espF / C-F*: CCGGAATTCGCCACCATGTCTCGTCCGGCACCGCGCGCCCCCACC and *espF / C-R*: CGCGGATCCCCACCTCCCC amplified the *espF /C*. The PCR product was digested with EcoRI / BamH I restriction enzyme and T-linked to the pEGFP-N1 plasmid to generate pEGFP-EspF, pEGFP-EspF / N, and pEGFP-EspF / C plasmids. Sequencing verified the integrity of the constructed plasmids.

293T cells were cultured according to standard methods, and the cells were plated on 10 cm^2 culture dishes (NEST, Hong Kong, China). According to the manufacturer's instructions, the cells were transfected with pEGFP-EspF, pEGFP-EspF / N, pEGFP-EspF / C plasmids using Lipofectamine 3000 (Thermo, USA).

CoIP and Western Blot

We followed the instructions of the co-immunoprecipitation Pierce CoIP Kit 26149. We took 80 μl of the control agarose resin slurry and added 1 mg of the protein sample to remove the non-specifically bound proteins. Then we took 20 μl of AminoLink resin slurry into the spin column, added 15 μg IgG antibody (Abclonal)/Flag antibody (CST), and co-incubated the mixture for 1 h. The non-specifically bound protein was added to the spin column, left at 4°C overnight, washed three times with IP lysis, and then eluted the Flag / IgG protein complex with the eluent. The above samples were used for 10% SDS-PAGE electrophoresis for immunoblotting. The primary antibodies of rabbit anti-Flag (CST) and rabbit anti-SMC1 (CST) were added and incubated overnight at 4°C. After three washes with TBST, the corresponding secondary antibody was added, incubated at room temperature for 1 hour, and the bands were visualized using an ECL chemical solution.

Silver stain

We took out the polyacrylamide gel after electrophoresis, added 20 ml of fixing solution, and left the gel for 15 min on a shaker under gentle agitation. Twenty ml of sensitizer was added, and the gel was left under gentle agitation for 45 min. Then we added the staining solution for 30 min. After rinsing with pure water, a chromogenic solution was added, and the protein bands became evident. The chromogenic solution was quickly poured out, and a stop solution was added. We then cut out the different bands, added the elimination solution, and shook the samples. After confirming that the slice was colorless, we sent it to Huijun Biological Company (Guangzhou) for mass spectrometry.

Mass Spectrometry

The decolorizing solution was added to the slice, which was then washed with mass spectrometry water. The gel was ground, acetonitrile was added, the supernatant was removed, 50 ml of the enzymatic hydrolysis was added, and then the sample was incubated at 37°C for 6 h. Then, 0.1% formic acid water was added, and the sample was shaken for 5 min to make it fully swelled. Acetonitrile was added, and the sample was shaken for another 5 min. The sample was centrifuged, and the supernatant was recovered to be analyzed on a mass spectrometer.

Bacterial infections

EHEC O157: H7 EDL 933 was cultured in LB medium, *ΔespF* and *ΔespF / pespF* in LB broth medium containing kana antibiotics at 37°C for 12 hours, and the HT-29 cells were seeded in 10 cm^2 culture dishes. When the cells reached 95% confluence, the cellular monolayer was washed with PBS, and the HT-29 cells were infected with bacteria at an MOI = 100: 1, and incubated in a humidified incubator at 37°C and 5% CO_2 for 6 hours. Then, the medium was aspirated, the cells were gently washed with PBS, and the proteins were collected for immunoblotting.

Immunofluorescence

Vero cells were plated on a confocal dish (35 mm, NEST, Hong) and grown overnight. When the cells reached 50% confluence, the cells were transiently transfected with the pEGFP, pEGFP-EspF, pEGFP-EspF / N, and pEGFP-EspF / C vectors. After 48 hours, the cells were gently washed with PBS three times, then fixed in 4% paraformaldehyde for 15 min at room temperature, and blocked with 0.1% Triton X-100 for 30 min. The primary antibody was added, and the sample was incubated at 4°C overnight. The sample was washed with PBS three times, incubated with the secondary antibody for 30 min, and then DAPI was added for nuclear staining. Cellular colocalization was observed under an FV1000 confocal microscope (Olympus, Tokyo, Japan).

Bioinformatics Analysis

The DAVID online tool was used to analyze protein MFs, BPs, CCs, cell localization, and KEGG signaling pathways. Taking the DAVID database as a background reference, we used GO and KEGG enrichment analysis to analyze the interacting proteins. The statistical analysis was based on Fisher's exact test. We used STRING to analyze PPIs. Venn diagrams were used to examine each protein pathway annotation.

Declarations

Ethics approval and consent to participate

Not applicable.

Consent for publication

Not applicable.

Availability of data and materials

The datasets used and/or analyzed during this study available from the corresponding author on reasonable request.

Competing interests

The authors declare that they have no competing interests.

Funding

This research is supported by funding from the Natural Science Foundation of Guangdong Province (No.2018B030311063) and co-funded by the Guangzhou Health Care Collaborative Innovation Major Project (No.201704020219), administered by Southern Medical University.

Author contributions

MQF designed the study the research; MQF, YH and KNY conceived the methods; MQF, JL, JLW, JYL and XXL performed the experiments; MQF, BZ, WZ, QWZ and CSW discussed the data and wrote the paper.

Acknowledgments

We thank LetPub (www.letpub.com) for its linguistic assistance during the preparation of this manuscript.

References

1. Al, J. M. R. E., (2005) Epidemiology of Escherichia coli O157:H7 Outbreaks, United States, 1982–2002 - Volume 11, Number 4—April 2005 - Emerging Infectious Disease journal - CDC. **11**: 603-609.
2. Boye, E. & B. Grallert, (2019) eIF2α phosphorylation and the regulation of translation. *CURR GENET*.
3. Charpentier, X. & E. Oswald, (2004) Identification of the secretion and translocation domain of the enteropathogenic and enterohemorrhagic Escherichia coli effector Cif, using TEM-1 beta-lactamase as a new fluorescence-based reporter. *J BACTERIOL***186**: 5486-5495.
4. Dean, P., J. A. Scott, A. A. Knox, S. Quitard, N. J. Watkins & B. Kenny, (2010) The enteropathogenic E. coli effector EspF targets and disrupts the nucleolus by a process regulated by mitochondrial dysfunction. *PLOS PATHOG***6**: e1000961.
5. Dean, P., J. A. Scott, A. A. Knox, S. Quitard, N. J. Watkins, B. Kenny & G. T. Van Nhieu, (2010) The Enteropathogenic E. coli Effector EspF Targets and Disrupts the Nucleolus by a Process Regulated by Mitochondrial Dysfunction. *PLOS PATHOG***6**: e1000961.
6. Díaz-Díaz, A., D. Roca-Lema, A. Casas-Pais, G. Romay, G. Colombo, Á. Concha, B. Graña & A. Figueroa, (2020) Heat Shock Protein 90 Chaperone Regulates the E3 Ubiquitin-Ligase Hakai Protein Stability. *CANCERS***12**: 215.
7. Enerly, E., H. AHMADI, K. SHALCHIAN-TABRIZI & A. LAMBERTSSON, (2003) Identification and comparative analysis of the RpL14 gene from Takifugu rubripes. *HEREDITAS***139**: 143-150.
8. Gabay-Maskit, S., M. Schuldiner & E. Zalckvar, (2018) Validation of a yeast malate dehydrogenase 2 (Mdh2) antibody tested for use in western blots. *F1000research***7**.
9. Garber, J. J., E. M. Mallick, K. Scanlon, J. R. Turner, M. S. Donnenberg, J. M. Leong & S. B. Snapper, (2018) Attaching-and-Effacing Pathogens Exploit Junction Regulatory Activities of N-WASP and SNX9 to Disrupt the Intestinal Barrier.
10. Gilson, P., G. Drouot, A. Witz, J. Merlin, P. Becuwe & A. Harlé, (2019) Emerging Roles of DDB2 in Cancer. *INT J MOL SCI***20**: 5168.
11. Hardwidge, P. R., I. Rodriguez-Escudero, D. Goode, S. Donohoe, J. Eng, D. R. Goodlett, R. Aebersold & B. B. Finlay, (2004) Proteomic Analysis of the Intestinal Epithelial Cell Response to Enteropathogenic Escherichia coli. *J BIOL CHEM***279**: 20127-20136.
12. Holmes, A., S. Muhlen, A. J. Roe & P. Dean, (2010) The EspF effector, a bacterial pathogen's swiss army knife. *Infection & Immunity***78**: 4445-4453.
13. Hua, Y., J. Ju, X. Wang, B. Zhang, W. Zhao, Q. Zhang, Y. Feng, W. Ma & C. Wan, (2018a) Screening for host proteins interacting withEscherichia coli O157:H7 EspF using bimolecular fluorescence complementation. *FUTURE MICROBIOL***13**: 37-58.
14. Hua, Y., J. Ju, X. Wang, B. Zhang, W. Zhao, Q. Zhang, Y. Feng, W. Ma & C. Wan, (2018b) Screening for host proteins interacting withEscherichia coli O157:H7 EspF using bimolecular fluorescence complementation. *FUTURE MICROBIOL***13**: 37-58.
15. Jackson, S. P. & J. Bartek, (2009) The DNA-damage response in human biology and disease. *NATURE***461**: 1071-1078.
16. Jefferson, M., B. Bone, J. L. Buck & P. P. Powell, (2020) The Autophagy Protein ATG16L1 Is Required for Sindbis Virus-Induced eIF2α Phosphorylation and Stress Granule Formation. *Viruses***12**: 39.

17. Kaper, J. B., (2005) Pathogenic Escherichia coli. *NAT REV MICROBIOL***295**: 355-356.
18. Kipanyula, M. J., P. F. S. Etet, L. Vecchio, M. Farahna, E. N. Nukenine & A. H. N. Kamdje, (2013) Signaling pathways bridging microbial-triggered inflammation and cancer. *CELL SIGNAL***25**: 403-416.
19. Kory, N., G. A. Wyant, G. Prakash, J. Uit De Bos, F. Bottanelli, M. E. Pacold, S. H. Chan, C. A. Lewis, T. Wang, H. R. Keys, Y. E. Guo & D. M. Sabatini, (2018) SFXN1 is a mitochondrial serine transporter required for one-carbon metabolism. *SCIENCE***362**: t9528.
20. Li, J., J. He, Y. Wang, Y. Shu & J. Zhou, (2019) SMC1 promotes proliferation and inhibits apoptosis through the NF-κB signaling pathway in colorectal cancer. *ONCOL REP***42**: 1329-1342.
21. Lidza, Kalifa, Jennifer, S., Gewandter, Rhonda, J., Staversky, Elaine & A., (2014) Kalifa L , Gewandter J S , Staversky R J , et al. DNA double-strand breaks activate ATM independent of mitochondrial dysfunction in A549 cells. *FREE RADICAL BIO MED*.
22. Luo, Y., X. Deng, F. Cheng, Y. Li & J. Qiu, (2013) SMC1-Mediated Intra-S-Phase Arrest Facilitates Bocavirus DNA Replication. *J VIROL***87**: 4017-4032.
23. M, M. & P. P, (2014) Enterohemorrhagic Escherichia coli as the cause of diarrhea in the Czech Republic, 1965-2013. *Epidemiologie, mikrobiologie, imunologie : casopis Spolecnosti pro epidemiologii a mikrobiologii Ceske lekarske spolecnosti J.E. Purkyne*.
24. Maddocks, O. D. K., A. J. Short, M. S. Donnenberg, S. Bader & D. J. Harrison, (2009) Attaching and Effacing Escherichia coli Downregulate DNA Mismatch Repair Protein In Vitro and Are Associated with Colorectal Adenocarcinomas in Humans. *PLOS ONE***4**.
25. Maddocks, O. D. K., K. M. Scanlon & M. S. Donnenberg, (2013) An Escherichia coli Effector Protein Promotes Host Mutation via Depletion of DNA Mismatch Repair Proteins. *MBIO***4**: e113-e152.
26. Marches, O., M. Batchelor, R. K. Shaw, A. Patel, N. Cummings, T. Nagai, C. Sasakawa, S. R. Carlsson, R. Lundmark & C. Cougoule, (2006) EspF of Enteropathogenic Escherichia coli Binds Sorting Nexin 9. *J BACTERIOL***188**: 3110-3115.
27. Mcnamara, B. P. & M. S. Donnenberg, (2006) A novel proline-rich protein, EspF, is secreted from enteropathogenic *Escherichia coli* via the type III export pathway . *FEMS MICROBIOL LETT***166**: 71-78.
28. Meyuhas, O., (2015) Ribosomal Protein S6 Phosphorylation: Four Decades of Research. *International Review of Cell & Molecular Biology***320**: 41.
29. Nagelkerke, A. & P. N. Span, (2016) *Staining Against Phospho-H2AX (γ-H2AX) as a Marker for DNA Damage and Genomic Instability in Cancer Tissues and Cells*. Springer International Publishing.
30. Nougayrède, J. P. & M. S. Donnenberg, (2004) Enteropathogenic Escherichia coli EspF is targeted to mitochondria and is required to initiate the mitochondrial death pathway. *CELL MICROBIOL***6**: 1097-1111.
31. Nougayrède, J. P., G. H. Foster & M. S. Donnenberg, (2007) Enteropathogenic Escherichia coli effector EspF interacts with host protein Abcf2. *CELL MICROBIOL***9**: 680-693.
32. Oliver, M., B. Miranda, S. Robert K, P. Amit, C. Nicola, N. Takeshi, S. Chihiro, C. Sven R, L. Richard, C. Celine, C. Emmanuelle, K. Stuart, C. Ian & F. Gad, (2006) EspF of enteropathogenic Escherichia coli binds sorting nexin 9. *J BACTERIOL***188**.
33. Pardal, A. J., F. Fernandes-Duarte & A. J. Bowman, (2019) The histone chaperoning pathway: from ribosome to nucleosome. *ESSAYS BIOCHEM***63**: 29-43.
34. Roxas, J. L., A. Koutsouris & V. K. Viswanathan, (2007) Enteropathogenic Escherichia coli-Induced Epidermal Growth Factor Receptor Activation Contributes to Physiological Alterations in Intestinal Epithelial Cells. *INFECT IMMUN***75**: 2316-2324.
35. Sawan, C. & Z. Herceg, (2010) Histone Modifications and Cancer. *ADV GENET***70**: 57-85.
36. Tahoun, A. S. G. S., (2011) Comparative Analysis of EspF Variants in Inhibition of Escherichia coli Phagocytosis by Macrophages and Inhibition of E. coli Translocation through Human- and Bovine-Derived M Cells. *INFECT IMMUN***79**: 4716.
37. Ti, S., G. M. Alushin & T. M. Kapoor, (2018) Human β-Tubulin Isotypes Can Regulate Microtubule Protofilament Number and Stability. *DEV CELL*.
38. Viswanathan, V. K., S. Lukic, A. Koutsouris, R. Miao & G. Hecht, (2004) Cytokeratin 18 interacts with the enteropathogenic Escherichia coli secreted protein F (EspF) and is redistributed after infection. *CELL MICROBIOL***6**: 987-997.
39. Viswanathan, V. K., S. Lukic, A. Koutsouris, R. Miao & G. Hecht, (2010) Cytokeratin 18 interacts with the enteropathogenic Escherichia coli secreted protein F (EspF) and is redistributed after infection. *CELL MICROBIOL***6**: 987-997.
40. Wang, X., Y. Du, Y. Hua, M. Fu, C. Niu, B. Zhang, W. Zhao, Q. Zhang & C. Wan, (2017) The EspF N-Terminal of Enterohemorrhagic Escherichia coli O157:H7 EDL933w Imparts Stronger Toxicity Effects on HT-29 Cells than the C-Terminal. *FRONT CELL INFECT MI***7**.
41. Weflen, A. W., N. M. Alto, V. K. Viswanathan & G. Hecht, (2010) E.coli secreted protein F promotes EPEC invasion of intestinal epithelial cells via an SNX9-dependent mechanism. *CELL MICROBIOL***12**: 919-929.
42. Yang, S., S. Hwang, M. Kim, S. B. Seo, J. Lee & S. M. Jeong, (2018) Mitochondrial glutamine metabolism via GOT2 supports pancreatic cancer growth through senescence inhibition. *CELL DEATH DIS***9**: 55.
43. Ying, Z., Y. Fei, W. Liang, W. Zhuo, Z. Naijin, W. Zhijun, L. Ziwei, S. Xiaoyu, W. Shi & C. Liu, (2018) Phosphorylation of SMC1A promotes hepatocellular carcinoma cell proliferation and migration. *INT J BIOL SCI***14**: 1081-1089.
44. Zhang, Y., P. Wang, Q. Zhang, X. Yao & S. Yao, (2017) eIF3i activity is critical for endothelial cells in tumor induced angiogenesis through regulating VEGFR and ERK translation. *Oncotarget***8**.
45. Zhang, Y., X. Zhang, M. R. Fleming, A. Amiri, L. El-Hassar, A. A. Surguchev, C. Hyland, D. P. Jenkins, R. Desai & M. R. Brown, (2016) Kv3.3 Channels Bind Hax-1 and Arp2/3 to Assemble a Stable Local Actin Network that Regulates Channel Gating. *CELL*: S1633427006.
46. Zhao, S. Z. Y. W., (2010) The N-Terminal Domain of EspF Induces Host Cell Apoptosis after Infection with Enterohaemorrhagic Escherichia coliO157:H7. *PLOS ONE***8: e55164.**

Figures

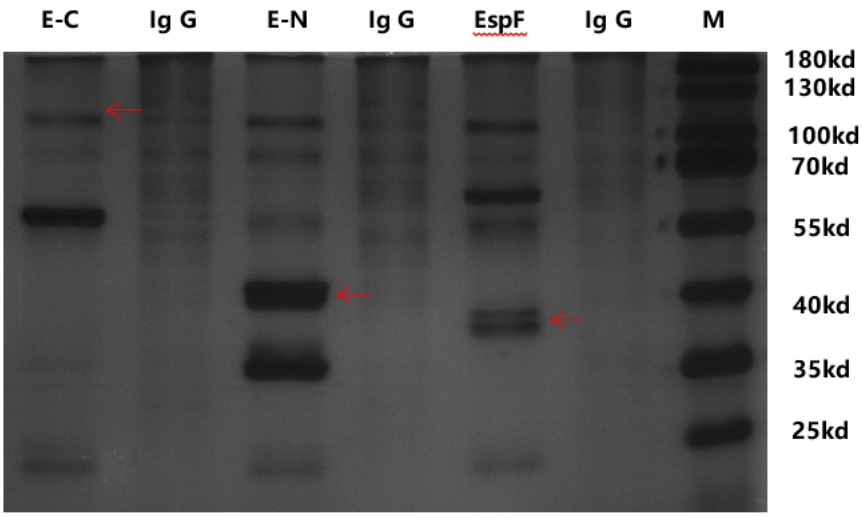

Figure 1

Silver staining of proteins. From left to right is the Maker, pEGFP-EspF/C Flag group and control group, the pEGFP-EspF / N Flag group and control group and , and the pEGFP-EspF Flag group and control group. The pEGFP-EspF, pEGFP-EspF-N, and pEGFP-EspF-C were tagged with 3x FLAG and were transfected into 293T cells. The proteins were lysed electroporated on an SDS-PAGE gel. The pEGFP-EspF group had two differential bands at 35-40 kDa, the pEGFP-EspF / N group had a differential band at 40 kDa, and the pEGFP-EspF / C group had a differential band at 130 kDa.

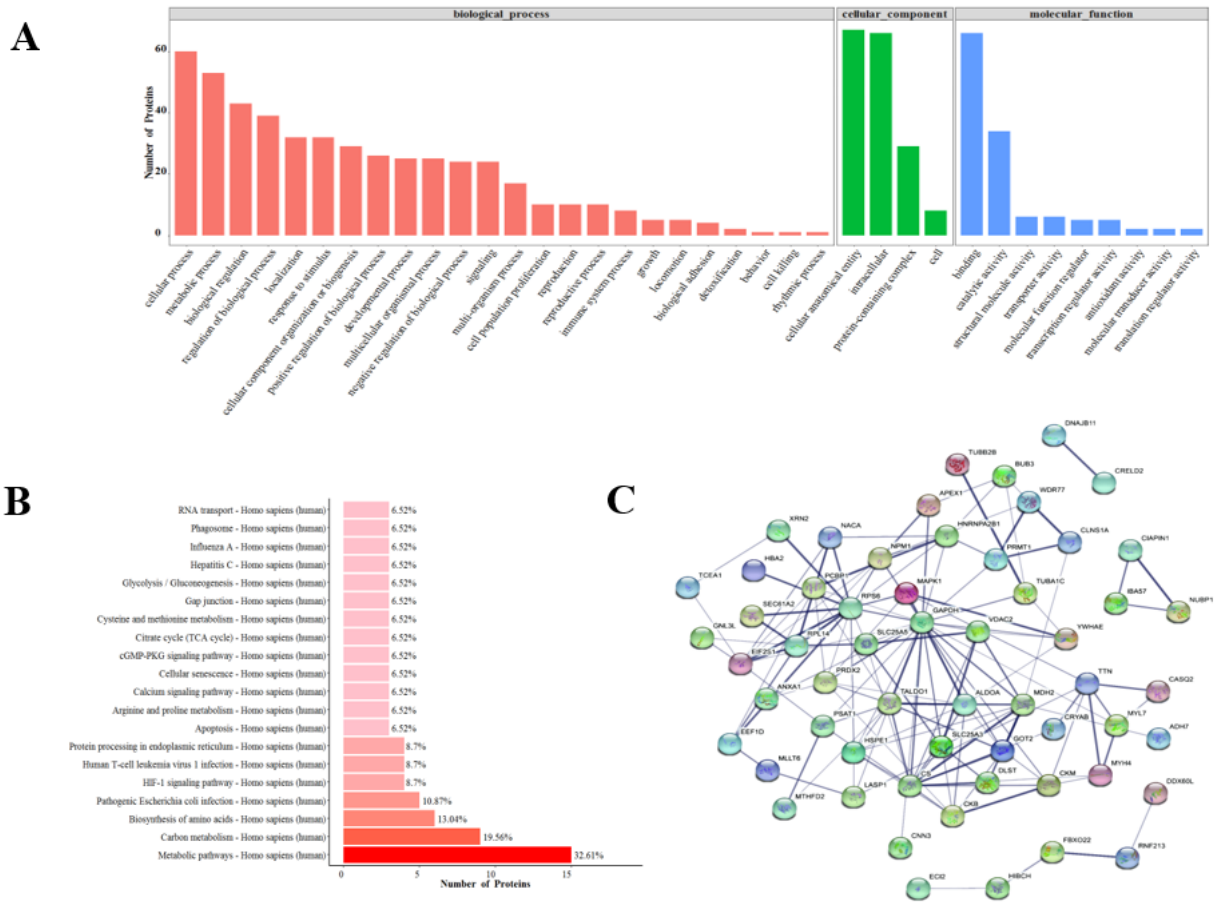

Figure 2

GO enrichment, KEGG pathway, and STRING analyses of the 38 kDa proteins interacting with EspF. (A) GO annotation of identified EspF-interacting proteins in biological processes, cell components, and molecular functions. (B) Genes and Genomes (KEGG) of the distribution of the top 20 interacting protein pathway. (C) STRING analysis of statistically significant proteins associated with the interacted proteins. The networks also illustrate the functional relationships (the edges) between the nodes; the thickness of the nodes is directly proportional to the association's significance score.

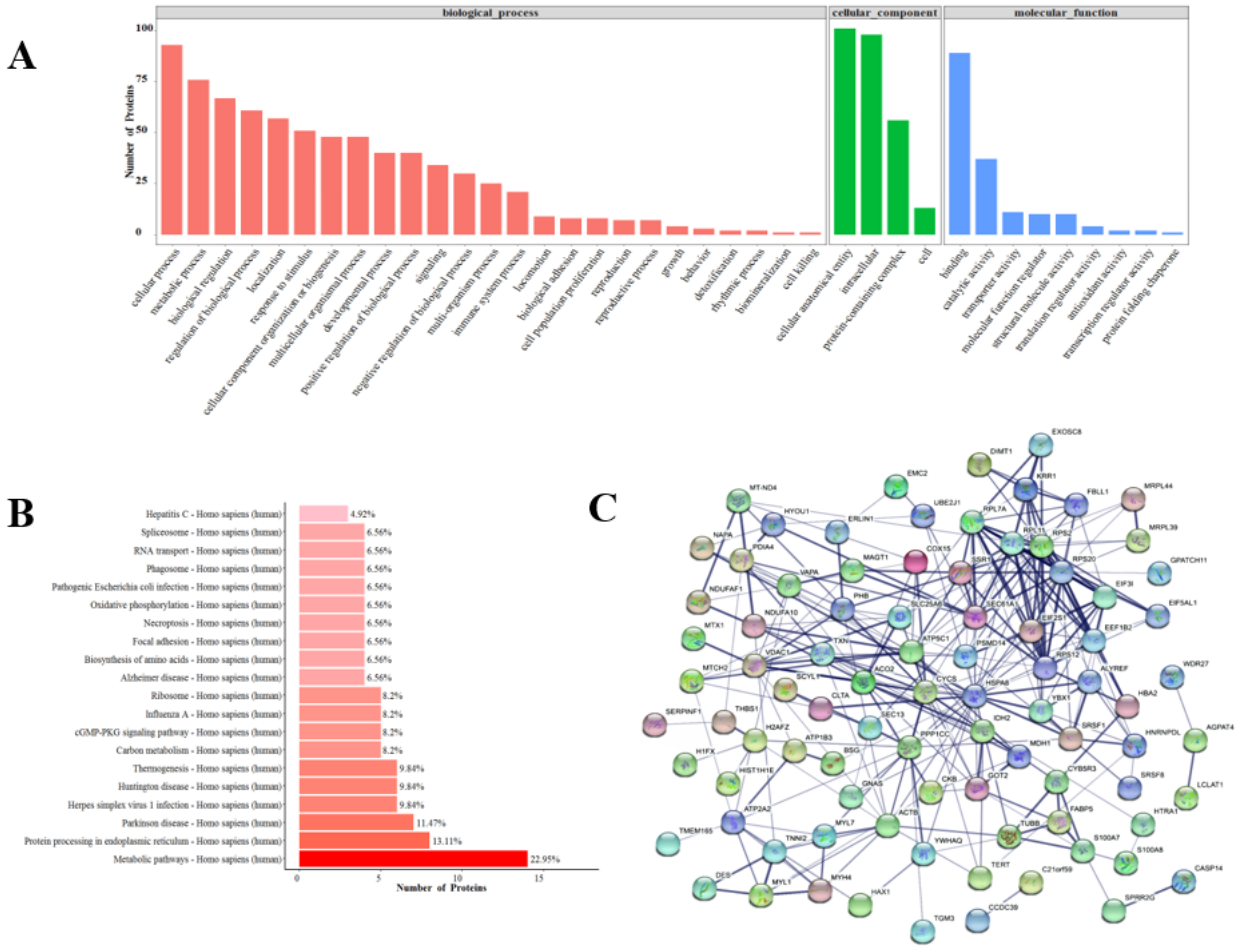

Figure 3

GO enrichment, KEGG pathway, and STRING analyses of the 36 kDa proteins interacting with EspF. (A) GO annotation of identified EspF-interacting proteins in BPs, CCs, and MFs. (B) KEGG of the distribution of the top 20 interacting protein pathways. (C) STRING analysis of statistically significant proteins detected in interacted proteins.

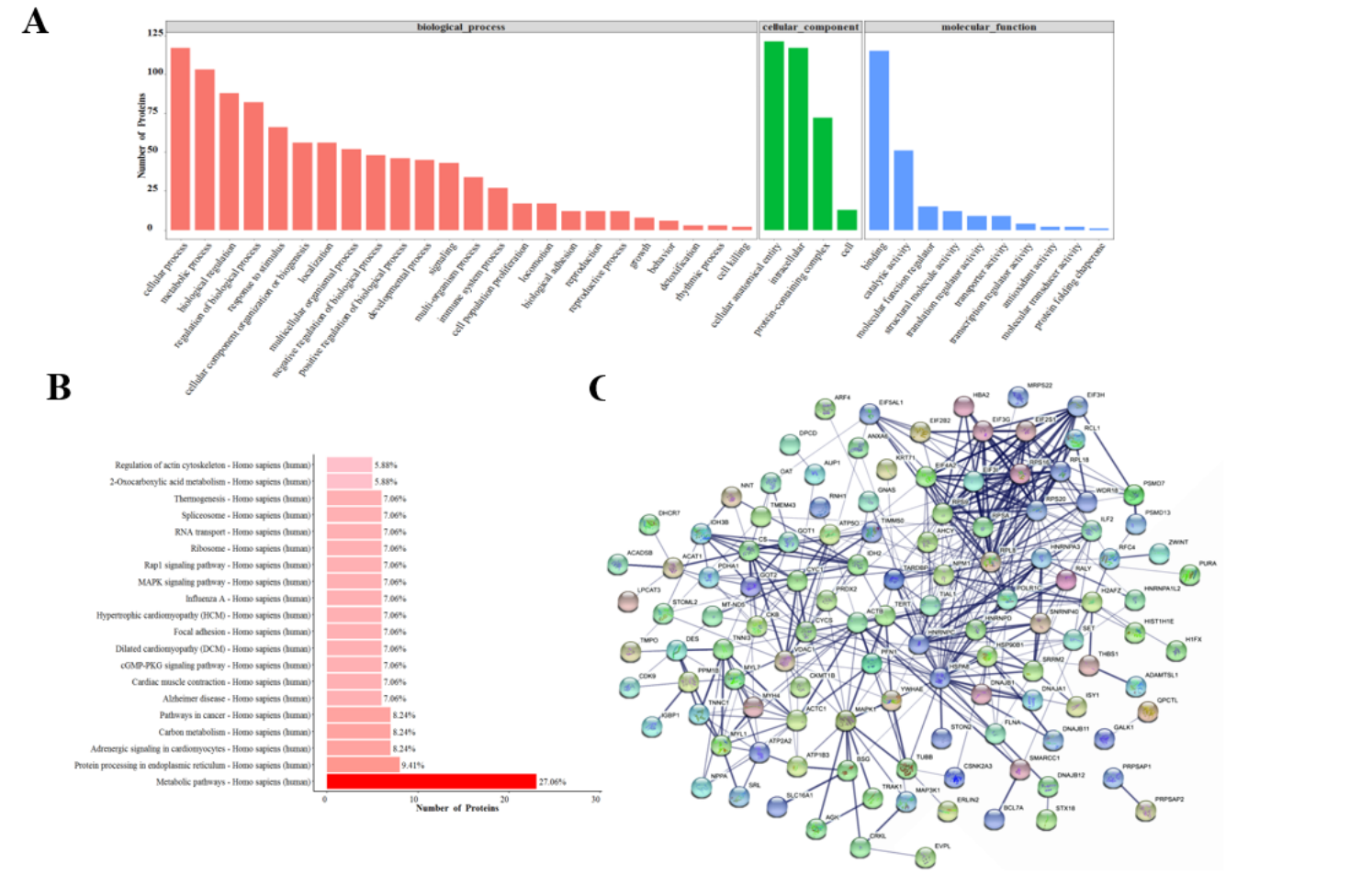

Figure 4

GO enrichment, KEGG pathways, and STRING analyses of the 40 kDa EspF-N terminus interacting proteins. (A) GO annotation of identified EspF-N terminus interacting proteins in BPs, CCs, and MFs. (B) KEGG of the distribution of the top 20 interacting protein pathways. (C) STRING analysis of statistically significant proteins detected in EspF-N-interacting proteins.

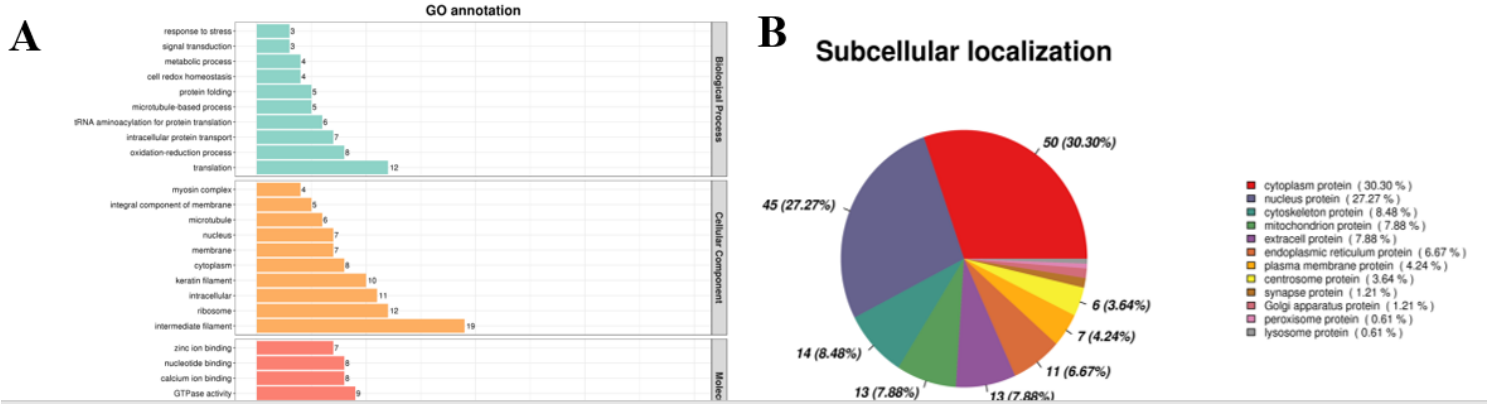

Figure 5

GO enrichment, KEGG pathways, and STRING analyses of the 130 kDa EspF-C terminus interacting proteins. (A) GO annotation of the identified EspF-C-interacting proteins in BPs, CCs, and MFs. (B) Subcellular location of the interacted protein. (C) KEGG of the distribution of the interacted protein pathways. (D) The COG function classification of the interacted protein (COG) pathways.

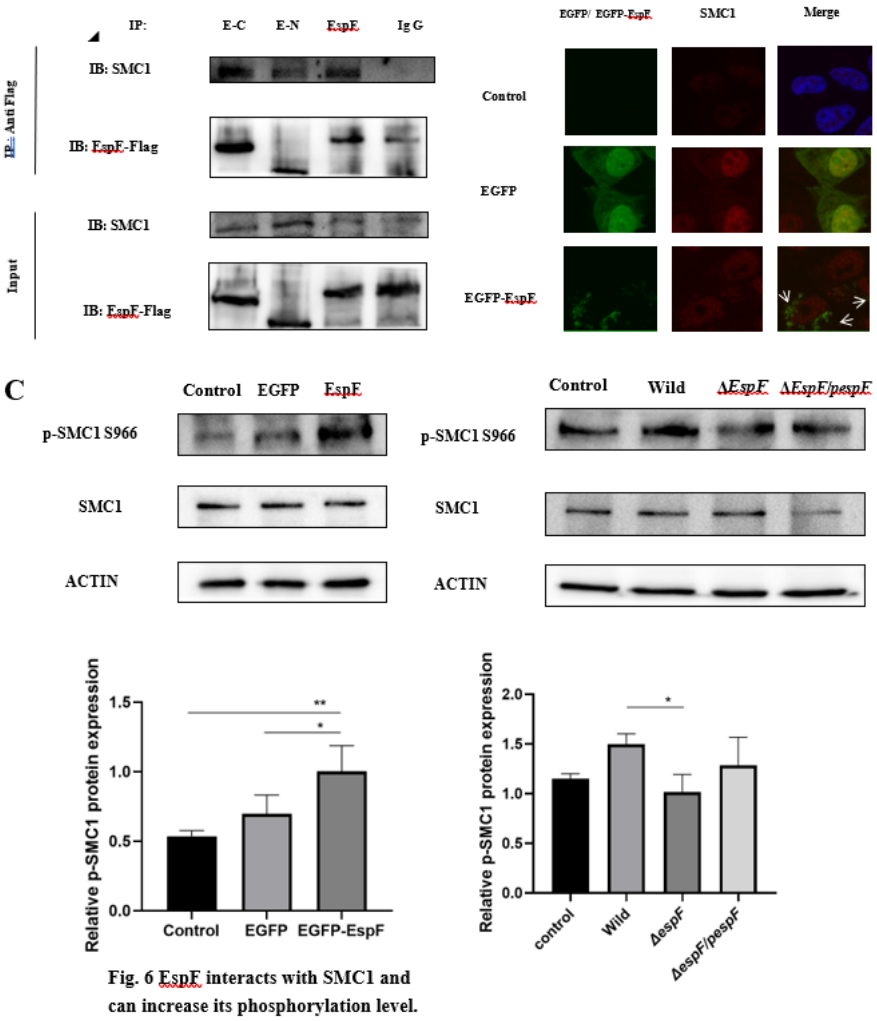

Fig. 6 EspF interacts with SMC1 and can increase its phosphorylation level.

Figure 6

EspF interacts with SMC1 and can increase its phosphorylation level. Co-immunoprecipitation to identify the interactions between SMC1 and EspF/EspF-N /EspF-C. The pEGFP-EspF, pEGFP-EspF-N, and pEGFP-EspF-C were tagged with 3x FLAG and were transfected into 293T cells. Cell proteins were extracted and incubated with Flag/IgG agarose beads. Then, the cell proteins (input) and the beads binding proteins were prepared for 10% SDS-PAGE. (B) Immunofluorescence to identify the interactions between EspF and SMC1. pEGFP-N1 and pEGFP-EspF were transfected into Vero cells. Then, the cells were incubated with anti-SMC1 antibody, and the colocalization was observed under a confocal microscope. The arrow points to co-location. (C) cells were transfected with pEGFP-N1/ pEGFP-EspF for 2 days or treated with strains for 6h and SMC1 and p-SMC1 expression was assessed by western blotting. ACTIN was used as loading control. Relative protein levels were quantified using Image J software. Data are shown as mean value±SD of three independent repeats. *P < 0.05, **P < 0.01.

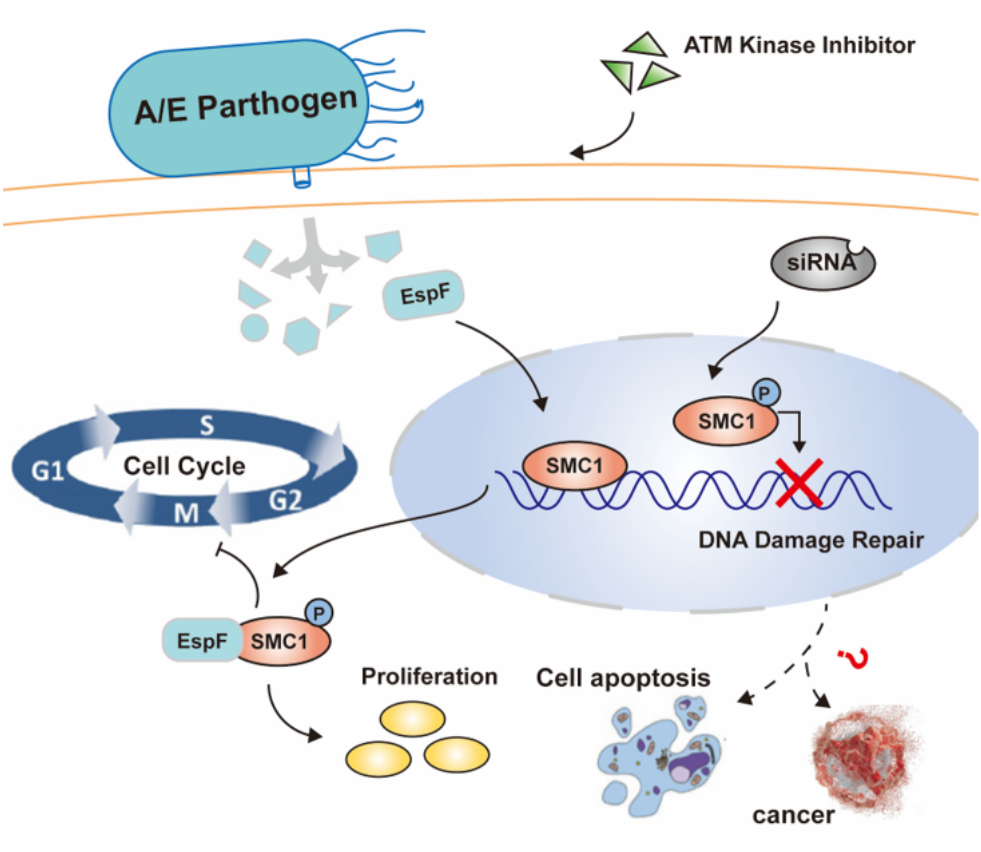

Figure 7

What is the biological effect of EspF mediated by SMC1? EspF can increase the expression of p-SMC1 and relocalize it in the cytoplasm. Therefore, EspF may mediate DNA damage, cell proliferation, cell cycle arrested, cell apoptosis, and even cancer by interacting with SMC1.

Supplementary Files

This is a list of supplementary files associated with this preprint. Click to download.

- 1.datacontrolREADME.txt
- allsample.xls
- stat.venn.svg
- COG.anno.png
- allsample.fa
- 2.1.GOREADME.txt
- COG.anno.pdf
- covprot.pdf
- 2.2.COGREADME.txt
- covprot.png
- COG.anno.cog2protein.xls
- GO.anno.go2protein.xls
- COG.anno.xls
- MSresultsofEspF36kDa.xlsx
- dmassdistri.pdf
- 2.3.KEGGREADME.txt
- dmassdistri.png
- 2.4.IPRREADME.txt
- GO.anno.xls

- GO.anno.pdf
- MSresultsofEspF38kDa.xlsx
- GOanalysis.xlsx
- 2.5.SubcellarREADME.txt
- IPR.anno.pdf
- MSresultsofEspFN40kDa.xlsx
- GO.anno.png
- GOKEGGCOG.anno.xls
- IPR.anno.png
- 2.6.statREADME.txt
- IPR.anno.ipr2protein.xls
- KEGG.anno.pdf
- Pathwayresults.xlsx
- lenprot.pdf
- KEGG.anno.png
- Peppro.xlsx
- 3.ProtExprQuantificationREADME.txt
- ppi.xlsx
- Flagusagedata.txt
- lenprot.png
- IPR.anno.xls
- lgGusagedata.txt
- KEGG.anno.ko2protein.xls
- MSresultsofEspF36kDaGOanalysis.png
- KEGG.anno.xls
- quality.xls
- MSresultsofEspF36kDapercent.png
- SMC1.txt
- MSresultsofEspF36kDaGOanalysis.pdf
- MSresultsofEspF36kDapercent.pdf
- Subcellular.localizationanno.xls
- MSresultsofEspF38kDaGOanalysis.pdf
- lgGmodification.xlsx
- MSresultsofEspF38kDaGOanalysis.png
- MSresultsofEspF38kDapercent.png
- MSresultsofEspF38kDapercent.pdf
- Flagmodification.xlsx
- MSresultsofEspF36kDa.pdf
- MSresultsofEspF38kDa.pdf
- MSresultsofEspFN40kDapercent.png
- MSresultsofEspFN40kDaGOanalysis.png
- MSresultsofEspFN40kDaGOanalysis.pdf
- MWdistri.png
- MWdistri.pdf
- stat.venn.png
- Subcellular.localization.pdf
- MSresultsofEspFN40kDapercent.pdf
- uniqdistri.pdf
- uniqdistri.png
- Subcellular.localization.png
- MSresultsofEspF38kDa.png
- MSresultsofEspFN40kDa.pdf

- MSresultsofEspF36kDa.png
- MSresultsofEspFN40kDa.png